Tellus SERIES B CHEMICAL AND PHYSICAL METEOROLOGY
PUBLISHED BY THE INTERNATIONAL METEOROLOGICAL INSTITUTE IN STOCKHOLM

Tellus (2008), 60B, 509–521
Printed in Singapore. All rights reserved

TELLUS

Observation of regional new particle formation in the urban atmosphere

By TAREQ HUSSEIN[1]*, JYRKI MARTIKAINEN[2], HEIKKI JUNNINEN[2], LARISA SOGACHEVA[2], ROBERT WAGNER[2], MIIKKA DAL MASO[2], ILONA RIIPINEN[2], PASI P. AALTO[2] and MARKKU KULMALA[2], [1]*Department of Applied Environmental Science, Stockholm University, SE-10691 Stockholm, Sweden;* [2]*Department of Physical Sciences, University of Helsinki, P.O. Box 64, FI-00014, Finland*

(Manuscript received 5 November 2007; in final form 7 April 2008)

ABSTRACT

Long-term measurements of fine particle number-size distributions were carried out over 9.5 yr (May 1997–December 2006), in the urban background atmosphere of Helsinki. The total number of days was 3528 with about 91.9% valid data. A new particle formation event (NPF) is defined if a distinct nucleation mode of aerosol particles is observed below 25 nm for several hours, and it shows a growth pattern. We observed 185 NPF events, 111 d were clear non-events and most of the days (around 83.5%) were undefined. The observed events were regional because they were observed at Hyytiälä (250 km north of Helsinki). The events occurred most frequently during spring and autumn. The observed formation rate was maximum during the spring and summer (monthly median 2.87 cm^{-3} s^{-1}) and the modal growth rate was maximum during late summer and Autumn (monthly median 6.55 nm h^{-1}). The events were observed around noon, and the growth pattern often continued on the following day. The observation of weak NPF events was hindered due to pre-existing particles from both local sources. It is clear that regional NPF events have a clear influence on the dynamic behaviour of aerosol particles in the urban atmosphere.

1. Introduction

Aerosol particles have direct and indirect impacts on the Earth's climate (e.g. Haywood and Boucher, 2000; Lohmann and Feichter, 2005) and public health (e.g. Atkinson et al., 1999; Künzli et al., 2000; Samet et al., 2000; Pope et al., 2002). Understanding the effects of aerosol particles requires detailed information on formation, transformation and removal processes in the atmosphere, in addition to their physical and chemical properties.

It has been remarked that new particle formation (NPF) have been observed in different kinds of environments including the free troposphere (e.g. Hoffman, 1993; Hoppel et al., 1994; Perry and Hobbs, 1994; Clarke et al., 1998, 1999a, b; Nyeki et al., 1999; Keil and Wendisch, 2001; Weber et al., 2001; Twohy et al., 2002), continental boundary layer such as northernmost sub-Arctic Lapland and remote boreal forest (Mäkelä et al., 1997; Vehkamäki et al., 2004; Kulmala et al., 2007), suburban and urban regions (Woo et al., 2001; Shi, 2003; Petäjä et al., 2007; Qian et al., 2007), industrialized agricultural areas (Birmili and Wiedensohler, 2000; Birmili et al., 2003), coastal environments around Europe (e.g. O'Dowd et al., 1999) and high mountains (Weber et al., 1995, 1996, 1997; Venzac et al., 2007). However, Most of these observations were either at a fixed point (i.e. platforms not necessarily moving along with the same air parcel) or they were limited for short time periods or few intensive measurement campaigns.

In fact, the observation of NPF on a regional scale is biased by the spatial variation of constituents in different air parcels. Furthermore, the observation at a single location is influenced by the existence of background aerosol particles. For example, aerosol particles larger than 100 nm in diameter, with relatively high number concentrations, enhance condensation and coagulation sinks and quickly removes the newly formed aerosol particles. Meteorological conditions such as turbulent fluctuations and air mixing, may also enhance NPF (e.g. Easter and Peters, 1994; Nilsson and Kulmala, 1998).

In this study, we are aiming to identify and analyse regional NPF events in the urban background of Helsinki during 5 May 1997–31 December 2006—a period of about 9.5 yr of fine particle number size distribution measurement. With the availability of previous classification of NPF events at another measurement station (SMEAR II, Hyytiälä located about 250 km north of Helsinki) in Southern Finland, we could identify the events as

*Corresponding author.
e-mail: tareq.hussein@helsinki.fi
DOI: 10.1111/j.1600-0889.2008.00365.x

regional or local. This study is a continuation of our analysis of the measured particle number size distributions in the Helsinki Metropolitan area, where we previously investigated the spatial-temporal variation of the particle number size distributions (e.g. Hussein et al., 2004, 2005b, 2007). According to our knowledge, this study includes the longest data set of the measured particle number size distributions in the urban background in Scandinavia and worldwide.

2. Methodology

2.1. Measurements and experimental setup

2.1.1. Measurement sites. Helsinki Metropolitan Area and its surrounding regions are situated on a fairly flat coastal area by the Baltic Sea at the latitude of 60°N. Because of the Gulf Stream and the prevailing global atmospheric circulation, the climate is relatively milder than other areas at the same latitudes. The Helsinki Metropolitan Area comprises four cities (Helsinki, Espoo, Vantaa and Kauniainen) with a total area of 743 km^2 and population of about 950 000 by the end of year 2001.

The particle number size distributions have been measured in Helsinki since 5 May, 1997. In this study, we considered the aerosol measurement until 31 December 2006. The aerosol measurement started at the old location of the Department of Physics of the University of Helsinki (Siltavuori campus). The 'Siltavuori campus' was located on a bank hill (Siltavuorenpenger), which is approximately 20-m high peninsula by the Baltic Sea. The campus was surrounded with urban sites including, the downtown at a distance of a few hundred metres to the southwest. Siltavuorenpenger is densely populated with residential and office buildings. The aerosol particle measurement took place at the ground level (about 1 m high) nearby the Department building.

In March 2001, the Department of Physics was re-located to its current location on the 'Kumpula campus'. The aerosol particle measurement was continued on the fourth floor of the department building. The Kumpula campus is located on a hilltop (∼20 m high from the nearby street level) about 5 km northeast of the Helsinki city downtown area. The campus was surrounded with residential buildings in the northeastern side and greenswards, mixed with houses, in the western side. At a distance of 200 m southeast, there was one of the major highways providing a significant source of traffic emissions. The area between the nearby highway and the campus was full of trees (about 10 m high) that efficiently shield a major part of the traffic emissions during the late spring, summer and early autumn, when the trees are full of leaves. A slight influence of traffic emissions on the measurement was usually observed during the winter season because of deciduous trees, which did not act as an active sink for ultrafine aerosol particles (Hussein et al., 2007).

In year 2004, the SMEAR III measurement station officially started, and the aerosol particle measurement was relocated within the Kumpula campus to join other on-site atmospheric and meteorological measurements. The aerosol measurement at the SMEAR III station was at ground level. The third of its kind in Finland (e.g. Hari et al., 1994; Vesala et al., 1998; Laakso et al., 2003; Vehkamäki et al., 2004; Dal Maso et al., 2005), the SMEAR-III measurement station has expanded the versatile atmospheric measurements to an urban area.

The first relocation from Siltavuori to Kumpula did not show significant differences on the physical characteristics of the measured particle number-size distribution; atmospheric aerosol particles showed clear urban background characteristics (Hussein et al., 2004, 2005b, 2006, 2007).

2.1.2. Measurement of particle number size distribution. Before year 2004, the particle number size distribution (dry diameter 7–500 nm) was measured with a differential mobility particle sizer (DMPS, e.g. Winklmayr et al., 1991; Aalto et al., 2001). The differential mobility analysis of aerosol particles relies on bipolar charging of aerosol particles (Liu and Pui, 1974), followed by classification of aerosol particles due to their electrical mobility by a differential mobility analyser (DMA, electrostatic Classifier TSI 3071, Knutson and Whitby, 1975) and then counting the particles with a condensation particle counter (CPC3025, TSI Inc., Shoreview, MN, USA) according to Stolzenburg and McMurry (1991) or (CPC 3010, TSI Inc.) according to Quant et al. (1992). The sample flow rate in the DMPS was 1.5 l min^{-1} and the sheath flow was 8.5 l min^{-1}, circulated back to the DMA after drying and filtering (Jokinen and Mäkelä, 1997; Birmili et al., 1999). The sheath flow dryer acted as a pulsation damper. The sampling line was approximately 2-m long Stainless Steel tube with 4-mm inner diameter. No special inlet was used—just a rain cover. The waiting time after the DMA voltage change was 15 s, after which the particle number concentrations were counted over a 3-s period. One measurement cycle took 5 min.

In year 2004, the DMPS was replaced with a twin-DMPS that covers a wider size range (dry diameter 3–950 nm). Contrary to a DMPS system, which consists of only one unit of differential mobility analyser, a twin-DMPS system consists of two differential mobility analysers. The first unit measured particle number-size distributions between 3 and 50 nm and it consisted of an ultrafine DMA (HAUKE-type, 10.9 cm in length) and an ultrafine CPC TSI 3025. The sample flow rate in this unit was 3 l min^{-1} and the sheath flow was 17 l min^{-1}. The second unit measured particle number size distributions between 10 and 950 nm with a DMA (HAUKE-type, 28 cm in length) and a CPC TSI 3010. The sample flow in this unit was 1.0 l min^{-1} and the sheath flow was 5 l min^{-1}. Each sheath flow was also arranged as a closed loop with a Topas aerosol dryer and an air filter. The sampling line was 2-m long metal tube with 4-mm inner diameter and the aerosol flow rate of 4 l min^{-1} was taken from a main inlet tube (flow rate of 60 l min^{-1}). One measurement cycle in the twin DMPS took about 10 min.

The particle number size distributions were extracted by data inversion. The inversion was done by using the MatLab

non-negative least squares (NNLS) algorithm. We used the transfer function of the classifier according to Stolzenburg (1988), and we defined the particle charging probability according to the semi-empirical functions by Wiedensohler (1989). We implemented laboratory calibrations for the CPC's detection efficiency. We estimated the losses in the transport lines and inside the DMA from the normal laminar flow tube diffusion loss equations.

The weekly maintenance of the DMPS system consisted of (1) aerosol and sheath flow rates calibration with a bubble flow meter and (2) the CPC zero was checked by turning the DMA voltage to zero. The yearly maintenance included CPC and DMA calibration and thorough cleaning. The CPC calibration included the particle detection efficiency calibration and the concentration calibration against an aerosol electrometer. The DMA calibration included transport loss calibration and the sizing accuracy calibration with PSL particles. The CPC was serviced and calibrated at the factory when needed.

2.2. Classification scheme

Our classification of NPF is based on the scheme described by Dal Maso et al. (2005), which was originally developed for remote regions. An NPF event is identified if a distinctly new mode of aerosol particles is observable in the nucleation mode size range (diameter < 25 nm) for, at least, several hours and it must show a growth pattern. An additional criterion is the possibility to quantify basic characteristics such as the particle growth rate (*GR*) and formation rate (J_{nuc}). Therefore, the evolving nucleation mode should be clearly distinguishable for a sufficient time period to ensure that we have enough data points for the quantitative analysis. Based on the accuracy of the quantitative analysis, there are two main classes of NPF events:

Class I: Both the growth rate and formation rate are determined with a good confidence level. This class is divided into two subclasses: Class Ia that illustrates clear and strong particle formation events with little or no pre-existing particles obscuring the observation of the newly formed mode; these cases are suitable for modelling studies. Class Ib contains the rest of cases.

Class II: the derivation of the growth rate and/or the formation rate was not possible or the accuracy of the results was questionable.

For comparison and control purposes while studying reasons leading to NPF events, time periods without NPF events are also of great interest. We identify days as 'non-events' whenever it is evident that no new particles is formed. However, many days do not fulfill the criteria for either an event or a non-event; instead 'undefined' is introduced here. In other words, 'undefined' class contains cases when some sporadic occurrence of newly formed particles in the nucleation mode size range is seen or when we clearly see the later phase of a mode growing in the Aitken mode size range without observing the newly formed mode below 25nm.

We classified the particle number size distributions visually on a daily basis. Days with missing data (and also inaccurate measurement) for a time period longer than 3 h during a day were removed from the data pool, because we cannot make sure that no particle formation is occurring during that period. However, if a day showed a clear NPF event, it was classified as such, despite the existence of gaps in the data.

2.3. Data analysis

2.3.1. Estimation of the growth rate and formation rate. The observed formation rate can be obtained from the flux of particles into the observable size range; that is, the time change rate of the measured particle number concentration of the smallest particle size. Typically, the actual formation rate (i.e. nucleation rate) is difficult to derive because the current instrumentation cannot measure the concentrations of aerosol particles smaller than 3 nm in diameter.

A critical part of a NPF event is the growth of the newly formed particles by condensation. The growth by condensation consumes a part of the condensable vapours from the atmosphere, and it can be a controlling mechanism, suppressing further particle formation. The growth process increases the particles' size so that they are less prone to removal by inter and intramodal coagulation. The particle growth might eventually progress to the Aitken mode size or even to the accumulation mode size, where they are likely to participate in cloud formation processes.

There are several methods to estimate the aerosol particle growth and formation rates (e.g. Weber et al., 1995; Mäkelä et al., 2000; Kulmala et al., 2001; Lehtinen and Kulmala, 2003): here we follow the approach by Dal Maso et al. (2005) because it is straightforward and it copes well with fluctuating data.

2.3.1.1. Growth rate (GR). The growth rate (*GR*) can be estimated by fitting the temporal variation of the geometric mean diameter of the newly formed particles (i.e. nucleation mode) to a first-order polynomial. If the nucleation mode does not show a well-behaved growth pattern, we choose a time period when the growth rate is nearly constant, preferably during the beginning of the NPF event. In the urban atmosphere, the result is expected to be influenced by pre-existing ultrafine particles (diameter $<$ 100 nm). On the other hand, if the estimation is limited to nucleation mode with small geometric mean diameters for which the growth rate is large, the newly formed aerosol particles grow quickly, and the growth rate estimation does not represent the new population in its entirety.

2.3.1.2. Formation rate $(J)_{\mathrm{nuc}}$. We define the observed formation rate (J_{nuc}) as the flux of the newly formed particles into the observable nucleation mode size range (Kulmala et al., 2004). To determine J_{nuc}, we assume a constant source of aerosol particles below the measurable size range, during a time period [$t_{1,\mathrm{start}}$,

$t_{1,\mathrm{end}}$]. The newly formed particles are expected to appear in the observable size range during a time period [$t_{2,\mathrm{start}}$, $t_{2,\mathrm{end}}$]. The time $t_{2,\mathrm{start}}$–$t_{1,\mathrm{start}}$ depends on the growth rate of the freshly formed particles below the observable particle size. During this time period, a fraction of the particles are lost due to coagulation. According to Dal Maso et al. (2005) J_{nuc} can be estimated as follows

$$J_{\mathrm{nuc}} = \frac{\mathrm{d}}{\mathrm{d}t} N_{\mathrm{nuc}} + F_{\mathrm{Coag}} + F_{\mathrm{growth}}, \tag{1}$$

where N_{nuc} is the nucleation mode particle number concentration, F_{Coag} is the loss rate of the nucleation mode particles due to coagulation and F_{growth} is the flux of particles out from the nucleation mode particle size range. Here we assume that the size range of the nucleation mode is below 25 nm in diameter.

Here we evaluate the nucleation mode particle number concentration (N_{nuc}) by directly integrating the measured number concentrations of aerosol particles

$$N_{\mathrm{nuc}} = \int_{D'_{\mathrm{p,min}}}^{25\,\mathrm{nm}} n_N(D'_{\mathrm{p}}) \cdot \mathrm{d}D'_{\mathrm{p}}, \tag{2}$$

where $D_{\mathrm{p,min}}$ is the smallest particle diameter in the measured particle number distribution $n_N(D_{\mathrm{p}})$. The nucleation mode number concentration can also be estimated from the multilognormal fitting of the particle number size distribution. In that case, we will denote the observed formation rate by J_{modal}.

The first term ($\mathrm{d}N_{\mathrm{nuc}}/\mathrm{d}t$) in eq. (1) is determined within the time period $t_{2,\mathrm{start}}$–$t_{2,\mathrm{end}}$, when the particle number concentrations of the nucleation mode (N_{nuc}) show a linear increase with time.

The second term (F_{Coag}) in eq. (1) can be calculated according to

$$F_{\mathrm{Coag}} = CoagS_{\mathrm{nuc}} N_{\mathrm{nuc}}, \tag{3}$$

where $CoagS_{\mathrm{nuc}}$ is the coagulation sink of the measured particle number-size distribution. Here we consider the reference size for the coagulation sink to be the geometric mean diameter of the nucleation mode, that is,

$$CoagS_{\mathrm{nuc}}(D_{\mathrm{p}})|_{D_{\mathrm{p}}=D_{\mathrm{pg,nuc}}} = \int_{D'_{\mathrm{p1}}}^{D'_{\mathrm{p2}}} K(D'_{\mathrm{p}}, D_{\mathrm{p}}) \cdot n_N(D'_{\mathrm{p}}) \cdot \mathrm{d}D'_{\mathrm{p}}, \tag{4}$$

where $K(D'_{\mathrm{p}}, D_{\mathrm{p}})$ is the coagulation coefficient of particles with diameters D_{p} and D'_{p} according to Fuchs (1964) and $n_N(D_{\mathrm{p}})$ is the measured particle number distribution [$\mathrm{d}N/\mathrm{d}(D_{\mathrm{p}})$].

The third term (F_{growth}) in eq. (1) represents the growth rate out of the nucleation mode according to

$$F_{\mathrm{growth}} = GR(D_{\mathrm{p}}) \cdot n_N(D_{\mathrm{p}})|_{D_{\mathrm{p}}=D_{\mathrm{p,max}}}, \tag{5}$$

where GR is the growth rate of the nucleation mode particles, $n_N(D_{\mathrm{p}})$ is again the measured particle number distribution [$\mathrm{d}N/\mathrm{d}(D_{\mathrm{p}})$] and $D_{\mathrm{p,max}}$ is the upper diameter of the nucleation mode, which is 25 nm here. The growth rate at the upper diameter of the nucleation mode during an intensive NPF event is typically small compared with $\mathrm{d}N_{\mathrm{nuc}}/\mathrm{d}t$ and F_{Coag}, therefore, F_{growth} can be neglected (Dal Maso et al., 2005).

2.3.1.3. Condensable vapour. The change rate of the condensable vapours in the atmosphere can be expressed mathematically according to

$$\frac{\mathrm{d}C}{\mathrm{d}t} = Q - CS \times C, \tag{6}$$

where C (molecules cm^{-3}) is the condensable vapour concentration in the atmosphere, Q (molecules $\mathrm{cm}^{-3}\ \mathrm{s}^{-1}$) is the condensable vapour source rate and CS (s^{-1}) is the condensation sink. At a steady-state condition, eq. (6) yields

$$Q = CS \times C. \tag{7}$$

Here, the concentration of the condensable vapour can be obtained from the growth rate of aerosol particles (Kulmala et al., 2001). In practice, the growth rate depends on the amounts of condensable vapours in the atmosphere. Assuming, the physical properties of the condensable vapours are similar to those of sulphuric acid and their pressure is higher than the saturation vapour pressure at the particle surface (Kulmala et al., 2001), the vapour concentrations (cm^{-3}) can be related to the growth rate (nm h^{-1}) according to

$$C = \frac{GR}{1.39 \times 10^{7}}. \tag{8}$$

The condensation sink (CS) in eq. (7) is estimated from the measured particle number size distribution

$$CS = 2\pi \sum_{D_{\mathrm{p}}} \beta(D_{\mathrm{p}}) \cdot D_{\mathrm{p}} \cdot N(D_{\mathrm{p}}), \tag{9}$$

where β is the transitional correction factor, D_{p} is the aerosol particle diameter and N is their number concentration.

2.3.2. Modal structure of the particle number size distribution: multilognormal fitting. The multilognormal distribution function, which is the sum of several lognormal modes, has been considered as the most suitable mathematical function to parametrize the particle number size distribution (e.g. Whitby, 1978). Each lognormal mode is defined by a geometric mean diameter (D_{pg}), a geometric standard deviation (σ_{g}) and a number concentration (N) as follows:

$$n_N^e(D_{\mathrm{p}}) \leftarrow \frac{\mathrm{d}N}{\mathrm{d}\log(D_{\mathrm{p}})} = \sum_{i=1}^{n} \frac{N_i}{\sqrt{2\pi}\log(\sigma_{\mathrm{g},i})} \times \exp\left\{-\frac{[\log(D_{\mathrm{p}}) - \log(\bar{D}_{\mathrm{pg},i})]^2}{2\log^2(\sigma_{\mathrm{g},i})}\right\}, \tag{10}$$

where the left-hand side represents the measured particle number size distribution and the right-hand side is the multilognormal distribution function (e.g. Seinfeld and Pandis, 1998). Note that here the particle number size distribution defined by eq. (10) is

related to the particle number distribution [$n_N(D_p)$], which was introduced in eqs. (4), (5) and (9), according to

$$n_N(D_\mathrm{p}) \leftarrow \frac{\mathrm{d}N}{\mathrm{d}D_\mathrm{p}} = \frac{1}{D_\mathrm{p}} \frac{\mathrm{d}N}{\mathrm{d}\log(D_\mathrm{p})} \rightarrow \frac{n_N^e(D_\mathrm{p})}{D_\mathrm{p}}. \quad (11)$$

In this study, we used our automatic fitting algorithm (DO-FIT, Hussein et al., 2005a) to find the suitable number of modes needed to best fit the measured particle number-size distribution. We implemented the best-fit parameters ($D_{\mathrm{pg},i}$, $\sigma_{\mathrm{g},i}$, Ni) in the formation rate and growth rate analysis, as described in the previous section. We also used the best-fit parameters to extrapolate the measured particle number-size distributions to 1 μm for the coagulation sink estimation ($CoagS_{\mathrm{nuc}}$) in eq. (4).

2.3.3. Data on long-range transport (LRT). The available information about the LRT episodes in Helsinki was based on personal communications with the Helsinki Metropolitan Area Council (YTV). A LRT episode was identified if the $PM_{2.5}$ and PM_{10} concentrations (24-h moving average) exceeded 20 μg m^{-3} in the background atmosphere within and around the Helsinki Metropolitan Area; the LRT information was available for years 1999–2004, only because of the lack of data on PM concentrations.

3. Results and discussion

3.1. Occurrence of new particle formation (NPF) events

We investigated the particle number-size distributions looking for NPF events in the urban background atmosphere of Helsinki during 5 May 1997–31 December 2006 (Table 1). The total number of classified days is 3528 and the total number of days with missing or invalid/bad data was 286. The bad data was defined according to the quality assurance of the raw data. During the whole measurement period, we observed and classified 185 d with clear NPF events: 89 d were Class I events (Figs. 1 and 2) and 96 d were Class II events (Fig. 3). Only 111 d were classified as clear non-events. Most of the days (around 83.5%) were undefined. Figures 1–3 illustrate the characteristic behaviour of NPF events in Helsinki.

Compared to the classification previously performed for the Boreal forest site (SMEAR II, Hyytiälä) in Southern Finland by Dal Maso et al. (2005), each classified day as a NPF event (Class I or Class II) at Helsinki was also classified as an event (either Class I or Class II) at Hyytiälä except 4 d were non-events, 29 d were undefined and 10 d were ignored due to missing/bad data. In total, 142 d (about 77% of the all events observed in Helsinki) were events at both places, which indicate that these events were regional over Southern Finland. One should keep in mind that a day being classified as undefined still holds a probability of being an event day. We, therefore, believe that the number of NPF events in Helsinki can be as many as those observed elsewhere in Southern Finland, but their observation was less frequent, compared with Hyytiälä for example, due to pre-existing ultrafine particles (UFP, diameter $<$100 nm), which are typically from traffic emissions. Therefore, our observation of NPF events in Helsinki was limited to the strongest ones.

The annual variation of the NPF events remained rather constant (around 14 event yr^{-1}) until year 2003, after which the number of events increased suddenly (Fig. 4). This sudden increase in yearly number of events between years 2003 and 2004 is mainly due to improvements in the measurement setup, allowing observation of aerosol particles smaller than 8 nm in diameter. Even though the number of events was increasing in Hyytiälä until year 2003 (Dal Maso et al., 2005) and started to decrease after that (Riipinen, 2008), we have not seen this in Helsinki so far. Note that the improvements in the measurement setup also improved our observation for clear non-events, because the number of non-events has shown a clear increasing trend. Relocating the measurement from the Department of the Physics to the SMEAR III station within year 2004 also

Table 1. Classifications of new particle formation events at Helsinki and at Hyytiälä; total number of days is 3528

	Hyytiälä						Helsinki	
	Class Ia	Class Ib	Class II	Non-event	Undef.	Bad/Missing	Total (Helsinki)	Percentage (%) (Helsinki)
Helsinki								
Class Ia	6	2	1	0	1	0	*10*	*0.28%*
Class Ib	15	33	19	0	9	3	*79*	*2.24%*
Class II	15	34	17	4	19	7	*96*	*2.71%*
Non-event	0	2	7	36	55	11	*111*	*3.15%*
Undef.	48	246	353	937	1192	170	*2946*	*83.50%*
Bad / Missing	6	18	28	87	99	48	*286*	*8.11%*
Hyytiälä								
Total (Hyytiälä)	*90*	*335*	*425*	*1064*	*1375*	*239*		
Percentage (%) (Hyytiälä)	*2.55%*	*9.50%*	*12.05%*	*30.16%*	*38.97%*	*6.77%*		

To validate the comparison between both sites we picked up the same time period (5 May 1997–31 December, 2006). The numbers here represent days and the table reads left-to-right for Helsinki and up-to-down for Hyytiälä.

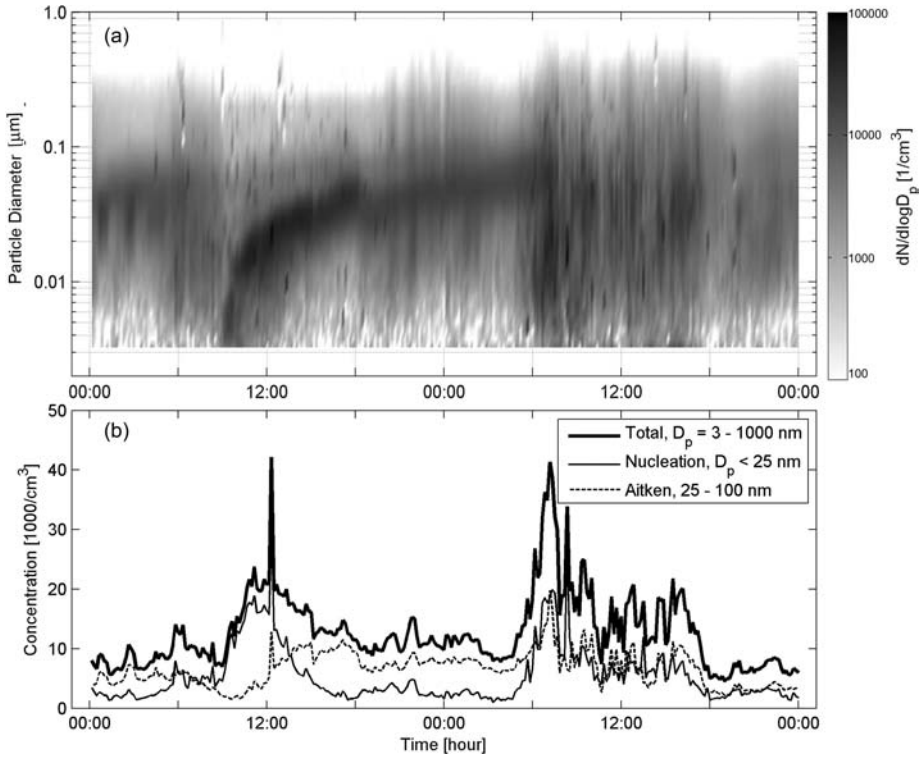

Fig. 1. An example of Class Ia event on 16 August 2004 (Monday) and the presuming growth pattern on the following day until the morning traffic rush hour (09:00): (a) particle number size distribution and (b) size-fractionated particle number concentrations. Class Ia events are characterized with accurate estimation of both the formation rate and the growth rate and they are good examples for modelling purposes.

improved the observation of clear non-events because the new location is obviously less influenced by the local emissions. These findings clearly indicate that the measurement setup does a have a clear influence on the observation of both NPF events and clear non-events days. It is therefore recommended for the purposes of observation of NPF events to measure aerosol particles down to the smallest possible diameter.

The NPF events (Classes I and II) in Helsinki had a clear annual pattern (Fig. 5): most of the events were during the spring (March–May) and autumn (September). The Class I events observed at both Helsinki and Hyytiälä (in total 56 events) were mainly during the spring and autumn periods, when the NPF event showed the highest probability at both places. This is expected because we believe that the observed events in Helsinki were regional over Southern Finland.

The NPF events in Helsinki also showed a clear pattern:

(1) The starting time of the event was, in general, around midday ±3 h when the nucleation mode particles suddenly increases.

(2) The newly formed particles grow rapidly to the Aitken mode size range (25–100 nm).

(3) The newly formed particles often continued their growth slowly within the Aitken mode size range, and they may reach to the accumulation mode size range slowly on the following days.

(4) The average time period elapsed from the starting moment to the moment of disappearance of the formed aerosol particles was less than 36 h.

The observed pattern of the NPF events in Southern Finland is quit similar to that observed elsewhere in the globe (see e.g. references listed in the introduction). They are often observed during daytime indicating that solar radiation and air mixing are probably important factors (e.g. Nilsson et al., 2001).

The NPF event clearly influences the dynamic behaviour of urban aerosol particles, especially when the amount of formed aerosol particles exceeds the background level. The influences of NPF events on the urban aerosol particles can be summarized as follows: (1) changing the daily pattern of the UFP number concentrations; (2) increasing the number concentrations during the nighttime of the event day and also during the early morning on the following day and (3) changing the modal structure of urban aerosol particles. Typically, the daily pattern of the urban aerosol particles, especially UFP, in Helsinki follows the daily patterns of the traffic density (Hussein et al., 2004).

We also investigated the occurrence of NPF events during LRT episodes. Our investigations revealed that all the observed NPF events in Helsinki did not occur during any of the identified LRT

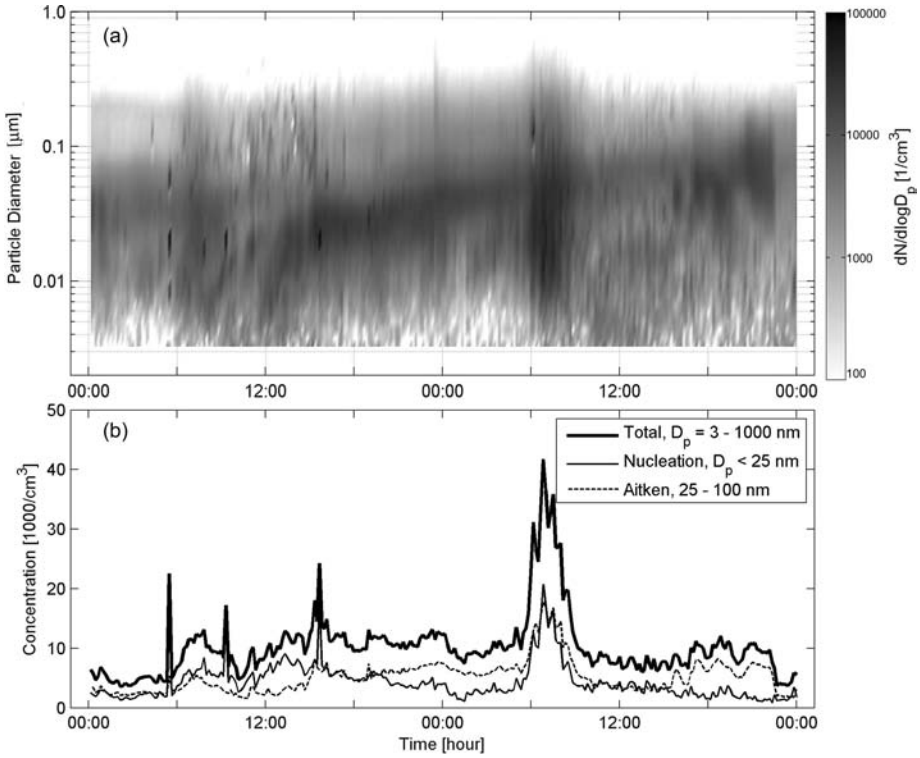

Fig. 2. An example of Class Ib event during 24 August 2004 (Tuesday) and the presuming growth pattern on the following day until the late evening: (a) particle number size distribution and (b) size-fractionated particle number concentrations. Class Ib events are characterized with accurate estimation of both the formation rate and the growth rate but they are not good examples for modelling purposes.

episodes. The existence of a LRT episode means that the number concentrations of particles larger than 100 nm in diameter are usually high, which provide high condensation and coagulation sinks that scavenge small particles efficiently and prevent them from being observed.

Based on the backtrajectory analysis with the HYSPLIT_4 model (Draxler and Hess, 1998), the arrival directions of air masses during NPF event, non-events and undefined days were clearly different from each others and, most importantly, different from air masses during LRT episodes. For example, during NPF events the air masses originated from northwest, whereas during non-events they originated from west and during undefined days from southwest.

3.2. Formation rate (J_{nuc})

Because the quantification of the formation rate and/or the growth rate was not satisfactory during Class II events due to data fluctuations, we limited our presentations of these quantities for Class I events only. At this stage, we shall recall again the difference between J_{nuc} and J_{modal}: both refer to the observed formation rate, but J_{nuc} is evaluated by using the integrated particle number concentration of the nucleation mode according to eq. (2) whereas J_{modal} is evaluated by using the nucleation mode particle number concentrations as estimated from the multilognormal fitting of the particle number-size distribution.

The mean value of the observed formation rate (J_{nuc}) during Class I events was about 2.4 cm^{-3} s^{-1} (median 1.8 cm^{-3} s^{-1}); the corresponding value, J_{modal}, was about 2.1 cm^{-3} s^{-1} (median 1.3 cm^{-3} s^{-1}). The monthly mean value of the J_{nuc} was maximum during April–July (Fig. 6 and Table 2). In general, the J_{nuc} at Helsinki is about three times its value at Hyytiälä. The mean value of the J_{nuc} at Hyytiälä was about 0.9 cm^{-3} s^{-1} (median 0.6 cm^{-3} s^{-1}). However, if we limit our comparison to the same events that occurred at the same time in both places, the monthly median of the J_{nuc} varies between 1.93 and 2.66 cm^{-3} s^{-1} in Helsinki and between 0.83 and 1.11 cm^{-3} s^{-1} in Hyytiälä (Table 2). The main reason for such difference between the two places is that J_{nuc} in the urban atmosphere represents the overall observed formation rate including both regional NPF and formations due to other sources such as primary and secondary emissions in the urban atmosphere.

3.3. Growth rate (GR)

The mean value of the *GR* during Class I events was about 3.8 nm h^{-1} (median 3.2 nm h^{-1}). The monthly mean value of the *GR* was maximum during July–September (Fig. 7). Even

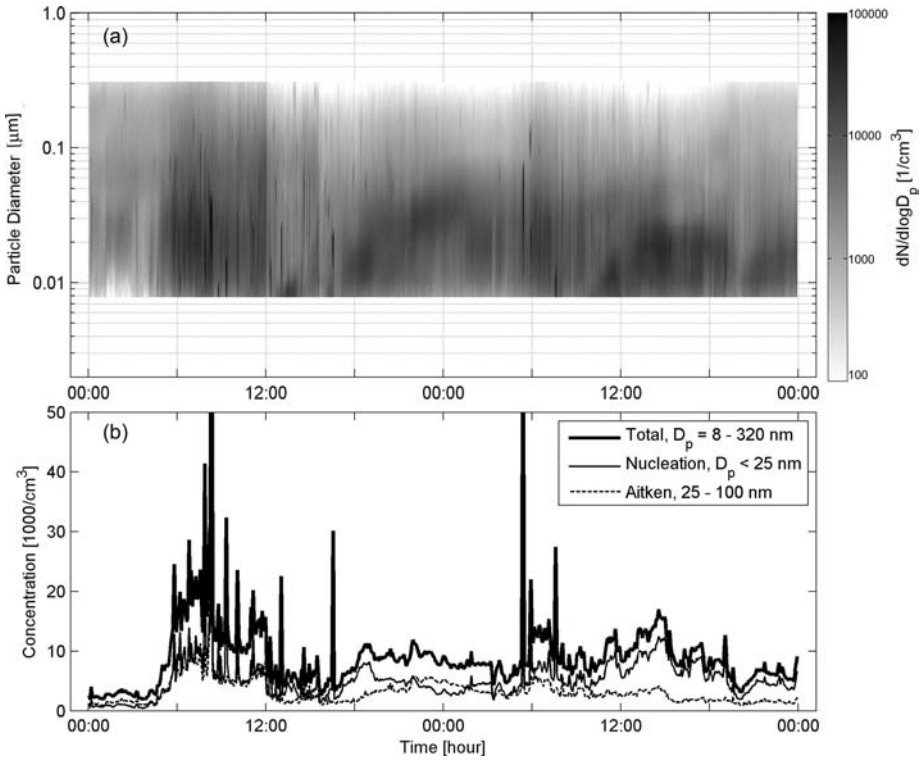

Fig. 3. An example of Class II event during 30 March 2004 (Tuesday) and the presuming growth pattern on the following day until the early morning: (a) particle number size distribution and (b) size-fractionated particle number concentrations. During Class II events, the formation rate and/or the growth rate are not well quantified; in this example, it was not possible to accurately quantify the formation rate due to the measurement limitation for particles smaller than 8 nm in diameter.

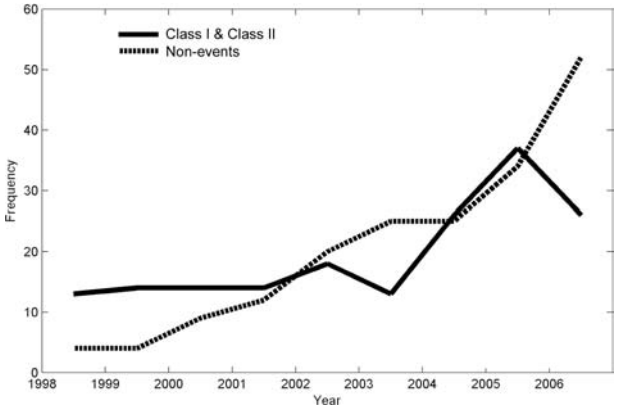

Fig. 4. Annual variation of non-events versus both Class I and Class II events in Helsinki during 1998–2006. The frequency here represents the total number of days per year.

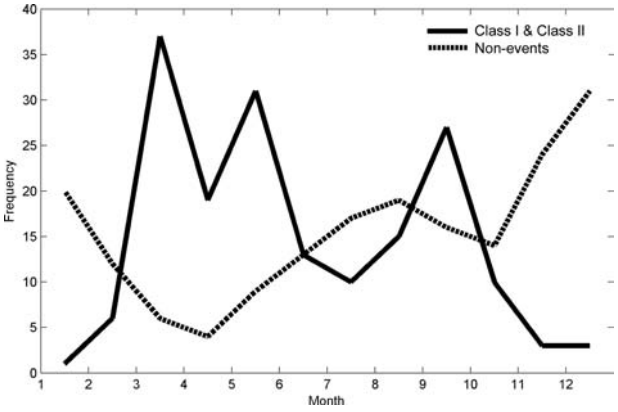

Fig. 5. Yearly pattern of non-events versus both Class I and Class II events in Helsinki during 1998–2006. The frequency here represents the total number of days per month. Note that we excluded the time period 5 May–31 December 1997 only to reserve the feature of the monthly variations.

though the observed NPF events were regional, the growth rate was slightly higher than that at Hyytiälä (Mena 3.0 nm h^{-1} and median 2.6 nm h^{-1}). If we limit our comparison to the same events that occurred at the same time in both places, the monthly median of the *GR* varies between 2.25 and 4.42 nm h^{-1} in Helsinki and between 1.67 and 3.62 nm h^{-1} in Hyytiälä (Table 3).

The differences between Helsinki and Hyytiälä regarding the *GR* estimation can be due to several reasons. First, it is expected to have high concentrations of condensable vapours in the urban atmosphere, which participate in the growth by condensation. Second, the number concentrations of UFP are also very high in

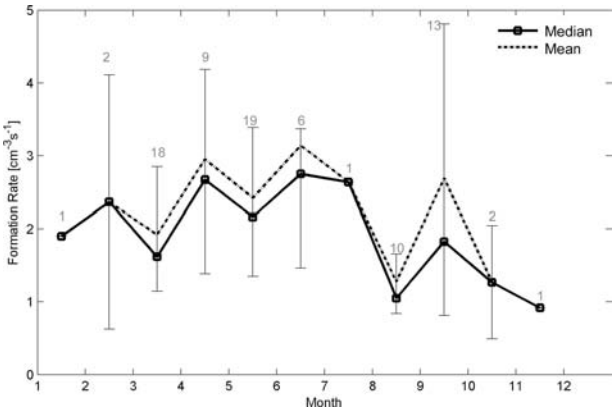

Fig. 6. Yearly pattern of the observed formation rate for Class I events in Helsinki during 1998–2006. The error bars represent the 25th and 75th percentiles and the numbers over the data point indicate the number of events used in the calculations for that month.

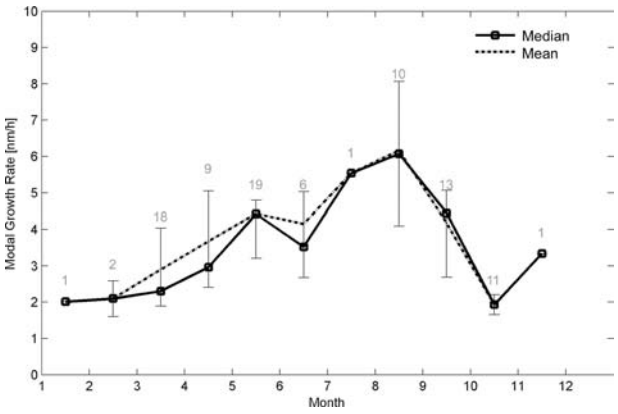

Fig. 7. Yearly pattern of the growth rate for Class I events in Helsinki (1998–2006). The error bars represent the 25th and 75th percentiles and the numbers over the data point indicate the number of events used in the calculations for that month.

the urban atmosphere where they are likely participating in the growth by coagulation. Third, and most important, the estimation method has a personal influence when selecting the time period to be used for the growth rate.

3.4. Condensable vapour source rate (Q)

The monthly mean value of the condensable vapour source rate (Q) varied between 9.2×10^4 and 7.8×10^5 molecules cm^{-3} s^{-1} (Annual mean 2.9×10^5 molecules cm^{-3} s^{-1} and median 2.1×10^5 molecules cm^{-3} s^{-1}), and it had similar annual variation as that of the GR (Fig. 8), which is proportional to the GR according to eq. (8) (Fig. 9). The monthly mean value of the Q is expected to be higher in the urban atmosphere such as Helsinki (varied between 9.3×10^4 and 7.8×10^5 molecules cm^{-3} s^{-1}) than that at Hyytiälä (varied between 6×10^3 and 2.1×10^5 molecules cm^{-3} s^{-1}).

The above mentioned values of the Q were calculated by using the measured particle number-size distribution to estimate the condensation sink. The mean value of the condensation sink (CS) during the growth period of event days (Class I events only) was about 5.1×10^{-3} s^{-1} (median 4.6×10^{-3} s^{-1}), which corresponds to a characteristic vapour lifetime of about 3.27 min. The mean value of the CS during non-event days was about 12.3×10^{-3} s^{-1} (median 11.1×10^{-3} s^{-1}).

Table 2. Monthly values of the observed formation rate (cm^{-3} s^{-1}) during Class I events in Helsinki (5 May 1997–31 December 2006) compared with the same events observed in Hyytiälä

	Helsinki				Hyytiälä				
Month	Mean ± *SD*	25%	Median	75%	Mean ± *SD*	25%	Median	75%	Number of events
January	–	–	–	–	–	–	–	–	0
February	0.63	–	0.63	–	1.17	–	1.17	–	1
March	2.03 ± 1.12	1.15	1.77	3.04	0.77 ± 0.41	0.42	0.67	1.15	16
April	2.09 ± 1.36	0.93	2.08	2.67	1.11 ± 0.88	0.23	1.09	1.72	6
May	2.14 ± 1.40	1.23	1.87	2.62	0.92 ± 0.73	0.38	0.60	1.41	16
June	3.03 ± 1.66	1.81	2.87	4.30	0.55 ± 0.68	0.07	0.55	1.03	3
July	–	–	–	–	–	–	–	–	0
August	1.25 ± 0.36	1.03	1.09	1.52	0.30 ± 0.13	0.20	0.30	0.40	3
September	2.85 ± 2.47	0.66	2.24	4.53	0.90 ± 0.60	0.31	0.83	1.35	10
October	2.04	–	2.04	–	0.39	–	0.39	–	1
November	–	–	–	–	–	–	–	–	0
December	–	–	–	–	–	–	–	–	0

Note that the listed values in this table do not match Fig. 6 because here we selected the events that were observed at the same time in both Helsinki and Hyytiälä.

Table 3. Monthly values of the growth rate [nm h^{-1}] during Class I events in Helsinki (5 May 1997–31 December 2006) and compared to the same events observed in Hyytiälä

	Helsinki				Hyytiälä				
Month	Mean ± *SD*	25%	Median	75%	Mean ± *SD*	25%	Median	75%	Number of events
January	–	–	–	–	–	–	–	–	0
February	1.6	–	1.6	–	0.59	–	0.59	–	1
March	2.47 ± 0.95	1.86	2.17	2.69	2.08 ± 1.00	1.31	1.77	2.73	16
April	2.90 ± 1.19	2.39	2.56	3.77	2.50 ± 1.77	1.01	1.91	3.76	6
May	4.05 ± 1.27	3.08	4.24	4.68	3.23 ± 1.08	2.17	3.40	4.17	16
June	3.38 ± 0.44	3.12	3.15	3.71	4.46 ± 1.39	3.63	3.72	5.48	3
July	–	–	–	–	–	–	–	–	0
August	6.49 ± 3.89	3.56	6.55	9.40	3.88 ± 2.12	2.36	3.50	5.50	3
September	4.04 ± 1.54	2.68	3.73	4.77	3.23 ± 1.23	2.40	3.00	3.34	10
October	2.21	–	2.21	–	2.91	–	2.91	–	1
November	–	–	–	–	–	–	–	–	0
December	–	–	–	–	–	–	–	–	0

Note that the listed values in this table do not match Fig. 7 because here we selected the events that were observed at the same time in both Helsinki and Hyytiälä.

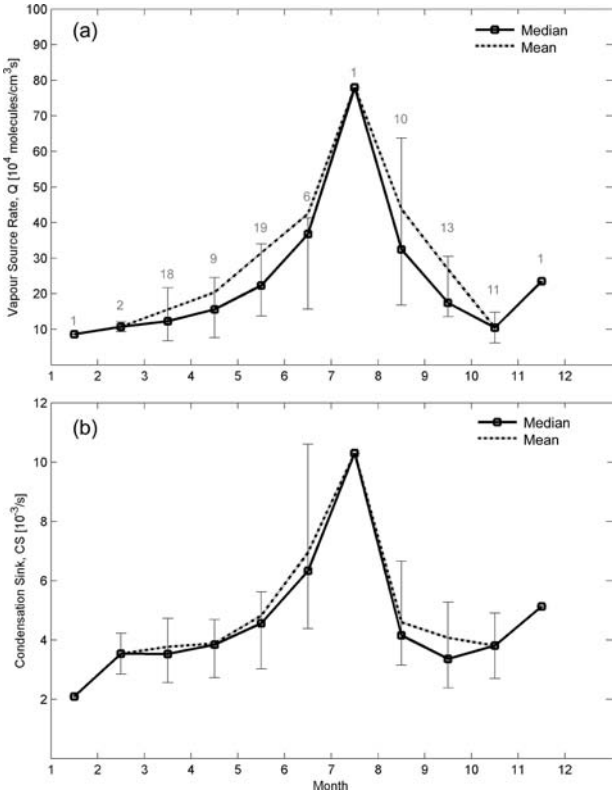

Fig. 8. Yearly pattern of (a) the condensable vapour source rate and (b) the condensation sink during Class I events in Helsinki (1998–2006). The error bars represent the 25th and 75th percentiles and the numbers over the data point indicate the number of events used in the calculations for that month.

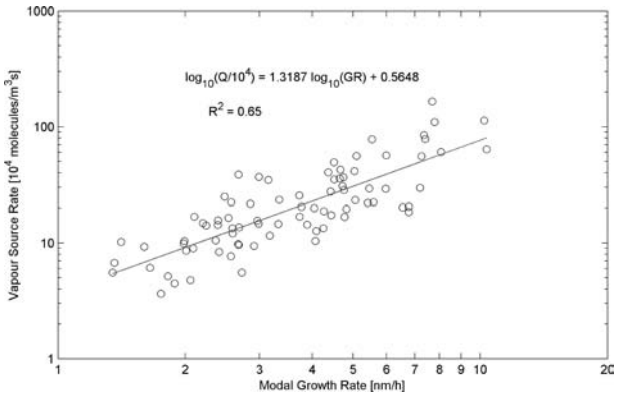

Fig. 9. Condensable vapour source rate (daily means) versus modal growth rate during Class I events (1998–2006).

However, the lower limit of the measured particle size range varied between 2 and 8 nm whereas the upper limit varied between 320 and 1000 nm. This variation was due to improvement in the experimental setup over time. It is therefore better to use the multilognormal fitting of the measured particle number-size distribution to estimate the *CS*. In this case, the mean value of the *CS* during the growth period of Class I events was around 6.1×10^{-3} s^{-1} (median 5.5×10^{-3} s^{-1}). This corresponds to a characteristic vapour lifetime of about 2.73 min and an average Q of 2.9×10^5 molecules cm^{-3} s^{-1} (median 2.1×10^5 molecules cm^{-3} s^{-1}).

4. Conclusions

We investigated the particle number-size distributions measured in the urban background of Helsinki during 5 May 1997–31

December 2006, looking for NPF events. We observed 185 clear NPF events: 89 were Class I and 96 were Class II. Only 111 d were clear non-event days and most of the days (around 83.5%) were undefined. Compared with NPF events observed at another location (Hyytiälä located about 250 km north of Helsinki) in Southern Finland, the observed NPF events in Helsinki were regional and their observation was limited to the strongest events only. The observation of weak NPF events in Helsinki was not possible due to pre-existing ultrafine particles (UFP, diameter < 100 nm) and also aerosol particles from LRT origin. Similar to NPF events observed elsewhere in Southern Finland, a clear annual pattern was observed in Helsinki. During NPF events the air masses originated from northwest, whereas during non-event days they originated from west and during undefined days from southwest.

The mean value of the observed formation rate (J_{nuc}) during Class I events was about 2.4 $\mathrm{cm}^{-3}\ \mathrm{s}^{-1}$ (median 1.8 $\mathrm{cm}^{-3}\ \mathrm{s}^{-1}$). The mean value of the growth rate (*GR*) during Class I events was about 3.8 nm h^{-1} (median 3.2 nm h^{-1}). Even though the observed NPF events were regional, both the J_{nuc} and the *GR* were slightly higher at Helsinki than those previously observed at Hyytiälä. This is mainly due to several reasons including high concentrations of condensable vapours and UFP particles in the urban atmosphere, where they enhance the growth by coagulation and condensation.

Referring to our previous analysis in the urban atmosphere of Helsinki and also other studies conducted elsewhere in other urban environments (e.g. Petäjä et al., 2007; Qian et al., 2007), regional NPF events have a clear influence on the dynamic behaviour of aerosol particles in the urban atmosphere.

As illustrated in this study, the measured size range of aerosol particles is a key factor in observing and quantifying NPF events in the urban atmosphere, it is recommended to set up the instrumentation to measure aerosol particle below 8 nm. On the other hand, pre-existing UFP also hinders the observation of the growth pattern of the newly formed particles. Pre-existing aerosol particles from LRT origin enhance the condensation and coagulation sinks and scavenge the newly formed particles quickly and prevent them from being airborne for a sufficient time to be observed.

Although the used classification scheme in this study is still valid for regional NPF events, a modified scheme is needed in the future to make it fully suitable for the urban atmosphere, especially to identify weak regional NPF events and also those that occur on a local scale. Moving toward that direction, the modified classification scheme should be extended to include the physical properties and dynamics of pre-existing aerosol particles.

References

Aalto, P., Hämeri, K., Becker, E., Weber, R., Salm, J. and co-authors. 2001. Physical characterization of aerosol particles during nucleation events. *Tellus* **53B**, 344–358.

Atkinson, R. W., Bremner, S. A., Anderson, H. R., Strachan, D. P., Bland, J. M. and co-authors. 1999. Short-term associations between emergency hospital admissions for respiratory and cardiovascular disease and outdoor air pollution in London. *Arch. Environ. Health.* **54**, 398–411.

Birmili, W. and Wiedensohler, A. 2000. New particle formation in the continental boundary layer: meteorological and gas phase parameter influence. *Geophys. Res. Lett.* **27**, 3325–3328.

Birmili, W., Stratmann, F. and Wiedensohler, A. 1999. Design of a DMA-based size spectrometer for large particle size range and stable operation. *J. Aerosol Sci.* **30**, 549–553.

Birmili, W., Berresheim, H., Plass-Dulmer, C., Elste, T., Gilge, S. and co-authors. 2003. The Hohenpeissenberg aerosol formation experiment (HAFEX): a long-term study including size-resolved aerosol, H_2SO_4, OH, and monoterpenes measurements. *Atmos. Chem. Phys.* **3**, 361–376.

Clarke, A. D., Davis, D., Kapustin, V. N., Eisele, F., Chen, G. and co-authors. 1998. Particle nucleation in the tropical boundary layer and its coupling to marine sulfur sources. *Science* **282**, 89–92.

Clarke, A. D., Kapustin, V. N., Eisele, F. L., Weber, R. J. and McMurry, P. H. 1999a. Particle production near marine clouds: sulfuric acid and predictions from classical binary nucleation. *Geophys. Res. Lett.* **26**, 2425–2428.

Clarke, A. D., Eisele, F., Kapustin, V. N., Moore, K., Tanner, D. and co-authors. 1999b. Nucleation in the equatorial free troposphere: Favorable environments during PEM-tropics. *J. Geophys. Res.* **104**, 5735–5744.

Dal Maso, M., Kulmala, M., Riipinen, I., Wagner, R., Hussein, T. and co-authors. 2005. Formation and growth of fresh atmospheric aerosols: eight years of aerosol size distribution data from SMEAR II, Hyytiälä, Finland. *Boreal Environ. Res.* **10**, 323–336.

Draxler, R. R. and Hess, G. D. 1998. An overview of the HYSPLIT_4 modeling system for trajectories, dispersion and deposition. *Aust. Meteorol. Mag.* **47**, 295–308.

Easter, R. C. and Peters, L. K. 1994. Binary homogeneous nucleation: temperature and relative humidity fluctuations, nonlinearity, and aspects of new particle production in the atmosphere. *J. Appl. Meteorol.* **33**, 775–784.

Fuchs, N. A. 1964. *The Mechanics of Aerosols*. Dover, New York .

Hari, P., Kulmala, M., Pohja, T., Lahti, T., Siivola, E. and co-authors. 1994. Air pollution in Eastern Lapland: challenge for an environmental measurement station. *Silva Fennica* **28**, 29–39.

Haywood, J. M. and Boucher, O. 2000. Estimates of the direct and indirect radiative forcing due to tropospheric aerosols: A review. *Rev. Goephys.* **38**, 513–543.

Hoffman, D. J. 1993. Twenty years of balloon-borne tropospheric aerosol measurements at Laramie, Wyoming. *J. Geophys. Res.* **98**, 12 753–12 766.

Hoppel, W. A., Frick, G. M., Fitzgerald, J. W. and Larson, R. E. 1994. Marine boundary layer measurements of new particle formation and the effects nonprecipitating clouds have on aerosol size distribution. *J. Geophys. Res.* **99**, 14 443–14 459.

Hussein, T., Puustinen, A., Aalto, P. P., Mäkelä, J. M., Hämeri, K. and co-authors. 2004. Urban aerosol number size distributions. *Atmos. Chem. Phys.* **4**, 391–411.

Hussein, T., Dal Maso, M., Petäjä, T., Koponen, I. K., Paatero, P. and co-authors. 2005a. Evaluation of an automatic algorithm for fitting the particle number size distributions. *Boreal Environ. Res.* **10**, 337–355.

Hussein, T., Hämeri, K., Aalto, P. P. and Kulmala, M. 2005b. Modal structure and spatial-temporal variations of urban and suburban aerosols in Helsinki area. *Atmos. Environ.* **39**, 1655–1668.

Hussein, T., Karppinen, A., Kukkonen, J., Härkonen, J., Aalto, P. P. and co-authors. 2006. Meteorological dependence of size fractionated number concentrations of urban aerosol particles. *Atmos. Environ.* **40**, 1427–1440.

Hussein, T., Kukkonen, J., Korhonen, H., Pohjola, M., Pirjola, L. and co-authors. 2007. Evaluation and modeling of the size fractionated aerosol particle number concentration measurements nearby a major road in Helsinki — Part II: aerosol measurements within the SAPPHIRE project. *Atmos. Chem. Phys.* **7**, 4081–4094.

Jokinen, V. and Mäkelä, J. M. 1997. Closed-loop arrangement with critical orifice for DMA sheath/excess flow system. *J. Aerosol Sci.* **28**, 643–648.

Keil, A. and Wendisch, M. 2001. Bursts of Aitken mode and ultrafine particles observed at the top of continental boundary layer clouds. *J. Aerosol Sci.* **32**, 649–660.

Knutson, E. O. and Whitby, K. T. 1975. Aerosol classification by electric mobility: apparatus, theory and applications. *J. Aerosol Sci.* **6**, 443–451.

Kulmala, M., Dal Maso, M., Mäkelä, J. M., Pirjola, L., Väkevä, M. and co-authors. 2001. On the formation, growth and composition of nucleation mode particles. *Tellus* **53B**, 479–490.

Kulmala, M., Vehkamäki, H., Petäjä, T. Dal Maso, M., Lauri, A. and co-authors. 2004. Formation and growth rates of ultrafine atmospheric particles: a review of observations. *J. Aerosol Sci.* **35**, 143–176.

Kulmala, M., Riipinen, I., Sipilä, M., Manninen, H. E., Petäjä, T. and co-authors. 2007. Toward Direct Measurement of Atmospheric Nucleation. *Science* **318**, 89–92.

Künzli, N., Kaiser, R., Medina, S., Studnicka, M., Chanel, O. and co-authors. 2000. Public-health impact of outdoor and traffic-related air pollution: a European assessment. *Lancet* **356**, 795–801.

Laakso L., Hussein T., Aarnio P., Komppula M., Hiltunen V. and co-authors. 2003. Diurnal and annual characteristics of particle mass and number concentrations in urban, rural and Arctic environments in Finland. *Atmos. Environ.* **37**, 2629–2641.

Lehtinen, K. and Kulmala, M. 2003. A model for particle formation and growth in the atmosphere with molecular resolution in size. *Atmos. Chem. Phys.* **3**, 251–258

Liu, B. Y. H. and Pui, D. Y. H. 1974. Electrical neutralization of aerosols. *J. Aerosol Sci.* **5**, 465–472.

Lohmann, U. and Feichter, J. 2005. Global indirect aerosol effects: a review. *Atmos. Chem. Phys.* **5**, 715–737.

Mäkelä, J. M., Aalto, P., Jokinen, V., Pohja, T., Nissinen, A. and co-authors. 1997. Observations of ultrafine aerosol particle formation and growth in boreal forest. *Geophys. Res. Lett.* **24**, 1219–1222.

Mäkelä, J. M., Dal Maso, M., Pirjola, L., Keronen, P., Laakso, L. and co-authors. 2000. Characteristics of the atmospheric particle formation events observed at a boreal forest site in southern Finland. *Boreal Environ. Res.* **5**, 299–313.

Nilsson, E.D. and Kulmala, M. 1998. The potential for atmospheric mixing processes to enhance the binary nucleation rate. *J. Geophys. Res.* **103**, 1381–1389.

Nilsson, E.D., Rannik, Ü., Kulmala, M., Buzorius, G., and O'Dowd, C.D. 2001. Effects of continental boundary layer evolution, convection, turbulence and entrainment, on aerosol formation, *Tellus B*, **53**, 441–461.

Nyeki, S., Kalberer, M., Lugauer, M., Weingartner, E., Petzold, A. and co-authors. 1999. Condensation Nuclei (CN) and ultrafine CN in the free troposphere to 12 km: a case study over the Jungfraujoch high-alpine research station. *Geophys. Res. Lett.* **14**, 2195–2198.

O'Dowd, C. D., McFiggans, G., Greasey, D. J., Pirjola, L., Hoell, C. and co-authors. 1999. On the photochemical production of new particles in the coastal boundary layer. *Geophys. Res. Lett.* **26**, 1707–1710.

Perry, K. D. and Hobbs, P. V. 1994. Further evidence for particle nucleation in clean air adjacent to marine cumulus clouds. *J. Geophys. Res. D* **99**, 22 803–22 818.

Petäjä, T., Kerminen, V.-M., Dal Maso, M., Junninen, H., Koponen, I. K. and co-authors. 2007. Sub-micron atmospheric aerosols in the surroundings of Marseille and Athens: physical characterization and new particle formation. *Atmos. Chem. Phys.* **7**, 2705–2720.

Pope, C. A. III, Burnett, R. T., Thun, M. J., Calle, E. E., Krewski, D. and co-authors. 2002. Lung cancer, cardiopulmonary mortality, and long-term exposure to fine particulate air pollution. *Am. Med. Assoc.* **287**, 1132–1140.

Qian, S., Sakurai, S. and McMurry, P. H. 2007. Characteristics of regional nucleation events in urban East St. Louis. *Atmos. Environ.* **41**, 4119–4127.

Quant, F. R., Caldow, R., Sem, G. J. and Addison, T. J. 1992. Performance of condensation particle counters with three continuous-flow designs. *J. Aerosol Sci.* **23**, S405-S408.

Riipinen, I. 2008. Observations on the first stes of atmospheric particle formation and growth. Report Series in Aerosol Science 95, Finnish Association for Aerosol Research (FAAR), Helsinki, Finland.

Samet, J., Dominici, F. C., Coursac, I. and Zeger, S. 2000. Fine particulate air pollution and mortality in 20 U.S. cities, 1987–1994. *New Eng. J. Med.* **343**, 1742–1749.

Seinfeld, H. S. and Pandis, S. N. 1998. *Atmospheric Chemistry and Physics: From Air Pollution to Climate Change* 2nd Edition. John Wiley & Sons, New York .

Shi, Q. 2003. *Continuous Measurements of 3 nm to 10 mm Aerosol Size Distributions in St. Louis*. MS Thesis. Department of Mechanical Engineering, University of Minnesota, Minneapolis, MN 55455 .

Stolzenburg, M. R. 1988. *An Ultrafine Aerosol Size Distribution System*. PhD thesis. University of Minnesota, Minneapolis, MN .

Stolzenburg, M. R. and McMurry, P. H. 1991. An ultrafine aerosol condensation nucleus counter. *Aerosol Sci. Technol.* **14**, 48–65.

Twohy, C. H., Clement, C. F., Gandrud, B. W., Weinheimer, A. J., Campos, T. L. and co-authors. 2002. Deep convection as a source of new particles in the midlatitude upper troposphere. *J. Geophys. Res.* **107**, doi: 10.1029/2001JD000323.

Vehkamäki, H., Dal Maso, M., Hussein, T., Flanagan, R., Hyvärinen, A. and co-authors. 2004. Atmospheric particle formation events at Värriö measurement station in Finnish Lapland 1998–2002. *Atmos. Chem. Phys.* **4**, 2015–2023.

Venzac, H., Sellegri, K. and Laj, P. 2007. Nucleation events detected at the high altitude site of the Puy de Dôme Research Station, France. *Boreal Environ. Res.* **12**, 345–360.

Vesala, T., Haataja, J., Aalto, P., Altimir, N., Buzorius, G. and co-authors. 1998. Long-term field measurements of atmosphere-surface interactions in boreal forest combining forest ecology, micrometeorology, aerosol physics and atmospheric chemistry. *Trends Heat, Mass Momentum Transfer* **4**, 17–35.

Weber, R. J., McMurry, P. H., Eisele, F. L. and Tanner, J. 1995. Measurement of expected nucleation precursor species and 3–500-nm diameter particles at Mauna Loa observatory, Hawaii. *J. Atmos. Sci.* **52**, 2242–2257.

Weber, R. J., Marti, J. J., McMurry, P. H., Eisele, F. L., Tanner, D. J. and co-authors. 1996. Measured atmospheric new particle formation rates: implications for nucleation mechanisms. *Chem. Eng. Commun.* **151**, 53–64.

Weber, R. J., Marti, J. J., McMurry, P. H., Eisele, F. L., Tanner, D. J. and co-authors. 1997. Measurements of new particle formation and ultrafine particle growth rates at a clean continental site. *J. Geophys. Res.* **102**, 4375–4385.

Weber, R. J., Moore, K., Kapustin, V., Clarke, A., Mauldin, R. L. and co-authors. 2001. Nucleation in the equatorial pacific during PEM tropics B: enhanced boundary layer H_2SO_4 but no particle production. *J. Geophys. Res.* **106**, 32 767–32 776.

Whitby, K. H. 1978. The physical characteristics of sulfur aerosols. *Atmos. Environ.* **12**, 135–159.

Wiedensohler, A. 1988. An approximation of the bipolar charge distribution for particles in the submicron size range. *J. Aerosol Sci.* **19**, 387–389.

Winklmayr, W., Reischl, G. P., Lindner, A. O. and Berner, A. 1991. A new electromobility spectrometer for the measurement of aerosol size distributions in the size range from 1 to 1000 nm. *J. Aerosol. Sci.* **22**, 289–296.

Woo, K. S., Chen, D. R., Pui, D. Y. H. and McMurry, P. H. 2001. Measurements of Atlanta aerosol size distributions: observations of ultra$ne particle events. *Aerosol Sci. Tech.* **34**, 75–87.